Journal of Thermal Analysis and Calorimetry, Vol. 81 (2005) 637–643

THERMAL AND DIELECTRIC STUDIES OF 2,2'-DIHYDROXYBENZOPHENONE
Progress of crystal nucleation and growth below the glass transition temperature

*S. Tomitaka, M. Mizukami, F. Paladi and M. Oguni**

Department of Chemistry, Graduate School of Science and Engineering, Tokyo Institute of Technology, O-okayama 2-12-1, Meguro-ku, Tokyo 152-8551, Japan

Thermal and dielectric properties of 2,2'-dihydroxybenzophenone were studied in relation with the potential progress of crystal nucleation and growth below the ordinary glass transition temperature, $T_{g\alpha}$. Differential scanning calorimetry was carried out in a range 100-350 K. The α glass transition was found to occur at $T_{g\alpha}$=239 K. Crystallization and fusion were observed to take place when the sample was cooled down to 103 K, but not observed when cooled to 203 K. Crystal nucleation was interpreted as having happened during annealing for a short time at 103 K which is much below the $T_{g\alpha}$. Heat capacities were measured in a range 7–350 K by an intermittent heating method with an adiabatic calorimeter. The temperature, enthalpy and entropy of fusion were determined to be 334.46 K, 20.07 kJ mol^{-1} and 60.01 J K^{-1}mol^{-1}, respectively. Crystal growth was found to proceed even at 220 K below the $T_{g\alpha}$, but no glass transition was detected below 220 K. Dielectric losses were measured in a temperature range of 100–250 K and a frequency range of 30 Hz–10 kHz. β-Relaxation process was found dielectrically with the activation energy of 22.6 kJ mol^{-1}, and the corresponding glass transition was expected to occur at 76.9 K. It is discussed, based on the "structurally ordered clusters aggregation" model for supercooled liquids and glasses, that the β process is potentially attributed to the crystal nucleation progressing at 103 K.

Keywords: *calorimetry, crystal growth, crystal nucleation, glass, glass transition, liquid structure, β relaxation*

Introduction

Molecules in the liquid state aggregate densely nearly to the same extent as in the crystalline state. Glass, being in the supercooled liquid phase, is in the freezing-in state with respect to the rearrangement of the molecules [1, 2]. While the molecules in the crystalline state are fixed in the ordered way as well, the mechanical and thermal properties of the glass are generally close to those of the crystal. The liquid/glass and crystal, however, have different structures in the arrangement of the molecules. In order for the liquid/glass to crystallize, therefore first a crystal nucleus, which is a small region with the same arrangement of molecules as that of bulk crystal, should be formed through the structural fluctuation of the liquid/glass [3, 4].

The ordinary crystal growth has been found to proceed in the range between the glass transition temperature, $T_{g\alpha}$, and fusion temperature, T_{fus}. The growth rate shows a maximum at a temperature, if anything, on the T_{fus} side, and gets almost zero at the $T_{g\alpha}$ [3, 4]. The latter is understood as the rearrangement rate of molecules becomes slower than the experimental time scale below the $T_{g\alpha}$ in accordance with the definition of a glass transition. We have found, however, a nucleation-based crystal growth proceeding in the $T_{g\alpha}$ region for the molecules with phenyl ring(s) [5–7]. In particular, the molecules with two phenyl rings have been observed to show rather large rates of the growth. *O*-benzylphenol and salol both with two phenyl rings, further, have been discovered to exhibit an anomalous phenomenon that the crystal nuclei appear, disappear, and reappear with time lapse at very low temperatures below the $T_{g\alpha}$ [8, 9]. The process proceeded even at 103 K which is lower by 130 K than the $T_{g\alpha}$ around 230 K. Why these compounds do such anomalous phenomena is not clear nor has been investigated both from the thermodynamic and kinetic aspects.

2,2'-Dihydroxybenzophenone (hereafter abbreviated as DHBP) is also a compound with two phenyl rings within the molecule. The crystal structure and the frequencies of intra-molecular normal vibration modes were determined [10, 11]. No thermal or crystallization properties have been, however, reported so far. In the present study, it was found in a differential scanning calorimetry (DSC) experiment that the compound also shows a phenomenon generating the crystal nuclei at 103 K as compared with $T_{g\alpha}$=239 K. Meanwhile, we have proposed a 'structurally ordered clusters aggregation' model as characterizing the structure of deeply supercooled liquids and glasses

* Author for correspondence: moguni@chem.titech.ac.jp

1388–6150/$20.00

Akadémiai Kiadó, Budapest, Hungary
Springer, Dordrecht, The Netherlands

[12, 13]. According to the model, the molecules within the structurally ordered regions (clusters) rearrange through the α process, and their rearrangement motion freezes below the $T_{g\alpha}$. On the other hand, the molecules in between the clusters can rearrange even below the $T_{g\alpha}$ and the molecular rearrangement is considered to construct a β-process. We therefore measured heat capacities of DHBP in the range 7–350 K by an adiabatic calorimetry and its dielectric losses due to a structural relaxation in the range 100–250 K. Attention was rather paid to the presence/absence of a β-relaxation process thereby to carry the crystal nucleation much below the $T_{g\alpha}$. A dielectric loss mode potentially connected to the β-relaxation was found but without detection of the corresponding calorimetric glass transition.

Experimental

Reagent grade of DHBP was purchased from Aldrich Co. Ltd., and purified by re-crystallization from methanol solution followed by sublimation (at 150°C)/deposition (at 0°C) processes. The purified sample was loaded into a DSC pan in air. The sample and the pan were renewed every cooling/heating cycle. The mass of the samples used was ca. 8 mg. Perkin-Elmer DSC-7 was utilized for the measurement. The sample of the same batch was loaded into a calorimeter cell under an atmosphere of helium gas. The mass of the sample used was weighed to be 8.012 g corresponding to 0.03740 mol. The heat capacities were measured by an intermittent heating method with a calorimeter reported already [14]. The inaccuracy and imprecision of the values obtained are expected to be less than ±0.3 and ±0.06% in the range 7–350 K.

The sample purified in the same procedure was loaded into a dielectrimetric cell of a concentric type under a He gas atmosphere: The thickness of the sample was 0.5 mm. The sample was cooled down to 100 K at 10 K min^{-1} to fall into the glassy state. The dielectric response was measured, on heating at a rate of 0.1 K min^{-1}, as a function of both temperature 100–250 K and frequency 30 Hz–10 kHz with employing an HP4284A LCR meter.

Results and discussion

DSC and crystal nucleation below the glass transition temperature

Figure 1 shows the DSC curves obtained. The sample loaded into a pan at room temperature was heated, as shown in Run 1, at a rate of 10 K min^{-1} up to 343 K to melt, and kept there for 2 min. Fusion occurred at

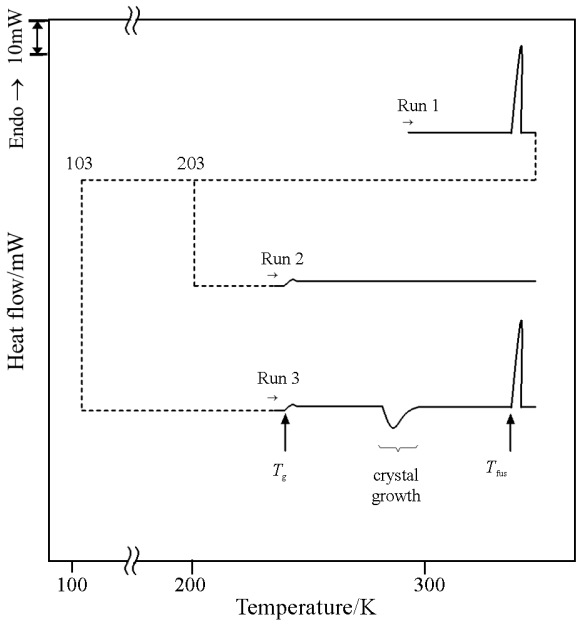

Fig. 1 DSC curves of 2,2'-dihydroxybenzophenone (DHBP): Run 1, sample as prepared; Run 2, sample rapidly cooled down to 203 K and heated up to 233 K at 200 K min^{-1}; Run 3, sample rapidly cooled down to 103 and heated up to 233 K at 200 K min^{-1}

334 K. Then it was cooled rapidly at 200 K min^{-1} down to 203 K, kept there for 1 min, heated at 200 K min^{-1} to 233 K, and kept there for 30 s. The measurement was then started in the heating direction at a rate of 10 K min^{-1}, and the result is depicted as Run 2. A glass transition was observed at 239 K as a shift in the baseline, but no other anomaly was observed. Run 3 was obtained by taking 103 K as the lowest temperature for cooling instead of 203 K for Run 2; The liquid sample was cooled from 343 K down to 103 K at a nominal rate of 200 K min^{-1}, kept there for 1 min, heated at 200 K min^{-1} to 233 K, and kept there for 30 s prior to a subsequent DSC measurement at 10 K min^{-1}. After the glass transition appeared at the same temperature as in Run 2, crystal growth occurred around 280 and fusion at 334 K. In view that crystal growth proceeds only in the presence of a crystal nucleus [3, 4] and that no crystallization is observed in the measurement cooled down to 203 K below 239 K, the progress of the crystal growth in Run 3 means that a crystal nucleation occurred during a cooling/heating cycle, experiencing the short annealing at 103 K below 203 K. 103 K is lower by 136 K than the $T_{g\alpha}$=239 K below which the rearrangement of the whole molecule is expected, from the ordinary understanding about the α glass transitions, to cease.

Heat capacities and determination of the purity of the sample

Figure 2 shows molar heat capacities: Filled circle, square, and open circle represent the results obtained for crystal, liquid, and glass, respectively. Part of the numerical values obtained is tabulated in Table 1. The heat capacities for supercooled liquid were measured in the heating direction after cooling the sample down to 285 K. The temperature dependence in 234–285 K was assumed by extrapolating linearly the data above 288 K as indicated with a dotted line. The values of crystal around the fusion were determined by extrapolating linearly the data in 280–310 K as indicated with a dot and dashed line. The heat capacity rise around 230 K in glass originates from a glass transition. The heat capacities of glass are rather constantly larger than those of crystal down to 7 K, indicating that the frequencies of some intermolecular vibrations are lower in the glass than in the crystal. However, no appreciable heat capacity jump or rise, which indicate presence of a β-glass transition, were found in the temperature dependence for the glass below 103 K.

Fusion enthalpy was measured by heating the crystal at a stretch from 320.279 to 338.401 K. The enthalpy and entropy of fusion were evaluated, taking the effect of fractional melting during the fusion into consideration for the heat capacity baseline, to be 20.07 kJ mol^{-1} and 60.01 J $K^{-1}mol^{-1}$, respectively. Figure 3 shows the temperature dependence of entropies evaluated assuming the third law of thermodynamics for crystal. The residual entropy was determined to be 23.63 J $K^{-1}mol^{-1}$. Kautzmann temperature, T_K, often thought to be the temperature at which

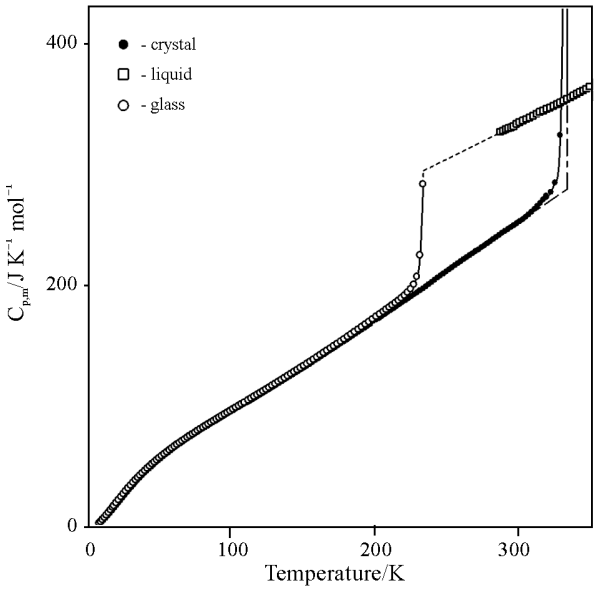

Fig. 2 Molar heat capacities of DHBP

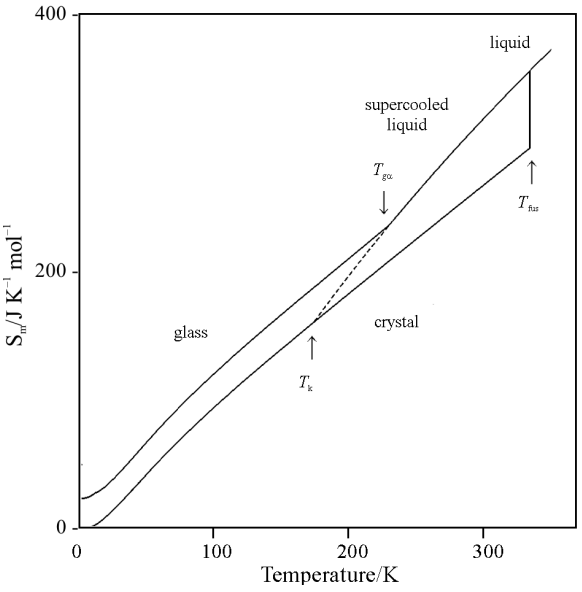

Fig. 3 Molar entropy curves of DHBP: The fusion and residual entropies are 60.01 and 23.63 J K^{-1} mol^{-1}, respectively

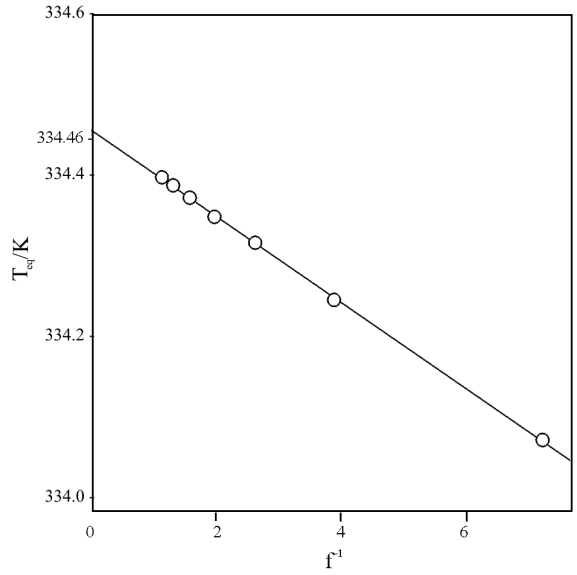

Fig. 4 Equilibrium temperature *vs*. the inverse of melt fraction of DHBP: The data are fitted well by a linear line indicating the presence of a liquid-soluble solid-insoluble impurity in the system

the molecular rearrangement ceases completely in the equilibrium liquid, was assessed to be 176.4 K, by extrapolating the heat capacities of supercooled liquid linearly *vs.* temperature below the $T_{g\alpha}$ [9]. Purity of the sample used was estimated by a fractional melting method. Figure 4 shows the equilibrium temperatures as a function of the inverse of the melt fraction. The dependence is well fitted by a linear line. The fusion temperature and purity of the sample were estimated from the dependence to be 334.46 K and 0.9989, respectively.

Table 1 Molar heat capacities of 2,2'-dihydroxybenzophenone

T/K	$C_{p,m}/R$	T/K	$C_{p,m}/R$	T/K	$C_{p,m}/R$	T/K	$C_{p,m}/R$
				Crystal			
8.72	0.4156	66.52	8.512	133.62	14.34	207.49	21.20
10.00	0.5696	68.23	8.691	135.52	14.51	209.53	21.40
11.42	0.7579	69.95	8.854	137.44	14.68	211.58	21.60
12.74	0.9573	71.67	9.017	139.36	14.85	213.62	21.78
14.17	1.186	74.00	9.177	141.28	15.02	215.66	21.98
15.69	1.441	75.13	9.335	143.22	15.19	217.69	22.18
17.32	1.718	76.86	9.495	145.16	15.37	219.73	22.37
18.85	1.985	78.60	9.654	147.11	15.54	221.77	22.58
20.29	2.238	80.35	9.811	149.06	15.71	223.80	22.76
21.67	2.483	82.10	9.961	151.02	15.89	225.84	22.96
23.00	2.719	83.86	10.12	152.99	16.06	227.88	23.16
24.43	2.974	85.62	10.27	154.97	16.24	229.92	23.35
26.03	3.254	87.37	10.42	156.95	16.44	231.96	23.55
27.64	3.532	89.14	10.57	158.94	16.63	234.00	23.74
29.18	3.795	90.90	10.72	160.94	16.81	236.04	23.95
30.66	4.039	92.67	10.87	162.93	16.99	238.08	24.16
32.09	4.272	94.45	11.03	164.93	17.17	240.12	24.38
33.47	4.490	96.24	11.19	166.93	17.36	242.16	24.60
34.83	4.701	98.04	11.34	168.93	17.55	244.20	24.82
36.36	4.933	99.85	11.49	170.93	17.73	246.24	25.02
38.06	5.183	101.67	11.64	172.94	17.92	248.28	25.22
39.71	5.414	103.50	11.80	174.95	18.11	250.32	25.43
41.31	5.632	105.34	11.95	176.97	18.30	252.36	25.64
42.88	5.838	107.19	12.10	178.98	18.48	254.41	25.85
44.42	6.037	109.05	12.27	181.00	18.67	256.45	26.06
45.93	6.226	111.05	12.41	183.03	18.86	258.49	26.25
47.55	6.442	113.05	12.56	185.05	19.05	260.54	26.45
49.29	6.648	114.89	12.72	187.08	19.25	262.58	26.66
51.05	6.859	116.74	12.87	189.12	19.45	264.63	26.85
52.79	7.064	118.59	13.03	191.16	19.63	266.68	27.05
54.52	7.262	120.45	13.19	193.70	19.86	268.72	27.45
56.24	7.452	122.31	13.35	195.23	20.02	270.77	27.25
57.96	7.641	124.18	13.52	197.28	20.22	272.83	27.60
59.67	7.824	126.06	13.68	199.32	20.52	274.88	27.83
61.38	8.002	127.94	13.85	201.37	20.65	276.93	28.02
63.09	8.176	129.82	14.01	203.41	20.80	278.99	28.22
64.80	8.348	131.72	14.17	205.45	21.00	281.04	28.42
283.09	28.64	295.43	29.83	307.76	31.09	320.09	32.96
285.15	28.84	297.49	30.02	309.81	31.35	323.21	33.32
287.20	29.05	299.54	30.22	311.87	31.63	326.18	34.27
289.26	29.26	301.60	30.43	313.93	31.93	329.76	38.98
291.31	29.45	303.65	30.61	315.98	32.23		
293.37	29.63	305.71	30.84	318.03	32.58		
				Glass and liquid			
7.82	0.4740	58.64	7.911	122.25	13.57	196.69	20.46
8.93	0.6145	60.42	8.096	124.35	13.76	198.73	20.71
10.22	0.8139	62.21	8.277	126.47	13.94	201.28	20.97
11.50	1.016	64.00	8.454	128.61	14.13	203.84	21.23
12.88	1.259	65.79	8.628	130.75	14.32	206.17	21.46
14.35	1.514	67.59	8.804	132.91	14.51	208.26	21.67
15.81	1.780	71.20	8.974	135.19	14.71	210.37	21.90
17.22	2.036	73.01	9.146	137.27	14.89	212.48	22.11
18.12	2.199	74.83	9.314	139.47	15.08	214.60	22.33
19.72	2.486	76.66	9.485	141.69	15.29	216.73	22.57
21.40	2.785	78.49	9.649	143.91	15.48	218.87	22.82
23.15	3.095	80.33	9.814	146.15	15.68	221.02	23.08
24.81	3.385	82.18	9.979	148.40	15.88	223.19	23.38
26.41	3.660	84.04	10.14	150.66	16.08	225.36	23.71
28.09	3.943	85.91	10.31	152.94	16.29	227.54	24.16
29.86	4.234	87.79	10.47	155.23	16.49	229.72	24.94

Table 1 Continued

T/K	$C_{p,m}/R$	T/K	$C_{p,m}/R$	T/K	$C_{p,m}/R$	T/K	$C_{p,m}/R$
			Glass and liquid				
31.56	4.506	89.68	10.79	157.54	16.71	231.88	27.08
33.20	4.760	91.58	10.96	159.85	16.95	233.97	34.12
34.80	4.996	93.19	11.12	162.18	17.16	236.18	53.64
36.35	5.220	95.41	11.29	164.52	17.38	288.03	39.28
38.00	5.454	97.34	11.45	166.88	17.60	289.94	39.40
39.76	5.690	99.29	11.62	169.25	17.82	291.84	39.53
41.46	5.916	101.05	11.78	171.63	18.05	293.73	39.63
43.13	6.132	103.22	11.95	174.03	18.28	295.63	39.72
44.77	6.341	105.20	12.12	176.44	18.51	297.52	39.85
46.38	6.544	107.19	12.29	178.87	18.74	299.40	40.08
47.97	6.739	109.20	12.45	181.30	18.98	301.51	40.25
49.67	6.944	111.29	12.69	183.75	19.22	303.87	40.39
51.48	7.143	113.94	12.86	186.22	19.46	306.22	40.55
53.27	7.340	115.99	13.04	188.70	19.70	308.57	40.70
55.06	7.532	118.07	13.22	191.19	19.96	310.93	40.87
56.85	7.724	120.15	13.40	193.69	20.20	313.29	41.08
315.65	41.25	325.12	41.85	334.63	42.54	343.65	43.22
318.02	41.39	327.50	42.01	337.01	42.69	345.89	43.39
320.38	41.54	329.87	42.18	339.17	42.88	348.12	43.55
322.75	41.69	332.25	42.36	341.42	43.05	350.36	43.78

Spontaneous heat evolution in the glass transition region

Figure 5 shows spontaneous heat evolution rates observed in the glass transition region in three series of heat capacity measurements: The samples in all the series were cooled rapidly at an average rate of 15 K min^{-1} in the glass transition region, and filled circle, open triangle, and open circle represent the results for the samples cooled down to 65, 65 and 7 K, respectively, before the measurements. Spontaneous heat evolution starts to be observed at around 180 K, and the rates are almost the same among the different series below 220 K, indicating that the dependence below 220 K is essentially due to the glass transition. The probable heat evolution effect only due to the glass transition is assumed as drawn with a dashed line, and the glass transition temperature, at which the relaxation time becomes 1 ks, is expected to be 235 K according to an empirical relation that the sample cooled rapidly at a rate in the order of 10 K min^{-1} shows a changeover from a heat evolution effect to an absorption one in the heating rate of about 0.1 K min^{-1} at the T_g [14, 15].

The temperature dependence of the rates above 220 K is quite different from that expected from the ordinary glass transition behavior and among the three different series even including the same lowest temperature of 65 K. The heat evolution rates above 235 K are too large to be expected from glass transition effects, and the sample turned to crystal after the completion of the evolution. This means that the abnormal heat evolution effects, which are different among the different series of measurements, are ascribed to crystallization. The effects, of course, originate from crystal growth, but not crystal nucleation. It is therefore indicated that crystal nucleation as a non-equilibrium, stochastic process proceeds at low temperatures and that the situation of crystal surfaces determining the volume rate of crystal growth is already different at 220 K every series of heat capacity measurements. 220 K is definitely lower than the calorimetric glass transition temperature.

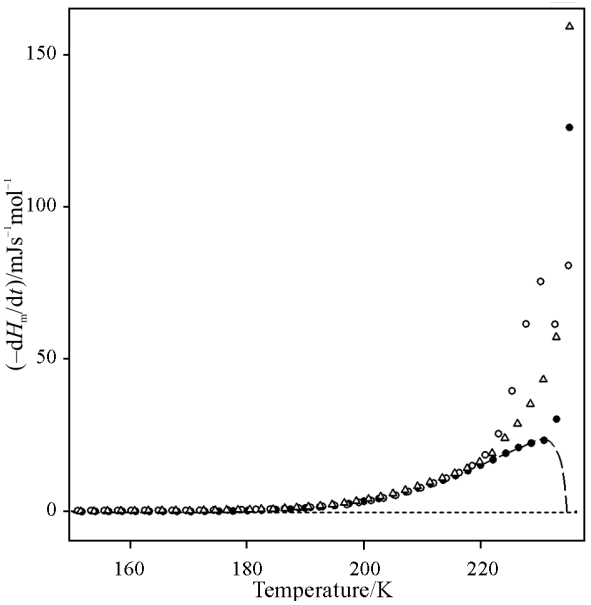

Fig. 5 Rates of the spontaneous heat evolution due to α glass transition and/or crystal growth: ●, Δ – sample cooled down to 65 K; ○ – sample cooled down to 7 K

Presence of a dielectric relaxation mode below the glass transition temperature

Figure 6 shows the results of dielectric relaxation loss, tanδ, in the glassy/liquid states. There is a relaxation mode, found clearly in 100–200 K below the calorimetric $T_{g\alpha}$=235 K, exhibiting a loss peak. Other two peaks are, in addition, found at around 230 and 240 K rather independently of the frequencies. The abrupt decrease in tanδ down to almost zero in 240–250 K is definitely ascribed to the crystal growth proceeding in the glass transition region of the liquid. However, why there should be double peaks at 230 and 240 K is not clear at present: In view that the frequencies of the measurements are higher than 0.1–1 mHz corresponding to the calorimetric time scale, the peak due to the α process, if in the case without the crystallization, should appear as a matter of course at higher temperatures than the $T_{g\alpha}$. The progress of the crystallization then results in extinction of the liquid phase in the sample and therefore extinction of the contribution of the α process to tanδ, leading to the consequence of the peak without frequency dependence. Nevertheless, there is no need to produce apparent two peaks.

Since a frequency-dependent loss peak was found in 100–200 K below the $T_{g\alpha}$, it is recognized potentially as originating from a β molecular rearrangement process. Figure 7 shows the Arrhenius plots of the relaxation times, τ_β, which were determined as the set of temperature and frequency, *f*, giving the peak and from a relation $\tau=2\pi f$. A fitting of the τ_β's by an Arrhenius equation, $\tau_\beta=\tau_{0\beta}\exp(\Delta\varepsilon_a/RT)$, gives an activation energy $\Delta\varepsilon_a$=22.6 kJ mol^{-1} and a pre-exponential factor $\tau_{0\beta}=4.3\times10^{-13}$ s. The $\tau_{0\beta}$ value is in a reasonable range as the frequency of a molecular vibration which leads to the relevant rearrangement of molecules, indicating the reasonableness of the fitting. The calorimetric glass transition is expected, if any, to occur at $T_{g\beta}$=76.9 K at which the relaxation time becomes 1 ks. The $T_{g\beta}$ is much lower than 103 K at which the sample was annealed for a short time in the DSC experiment and a crystal nucleus was recognized as formed through a certain molecular rearrangement. Thus it is probable that the nucleation is brought through the β rearrangement of molecules.

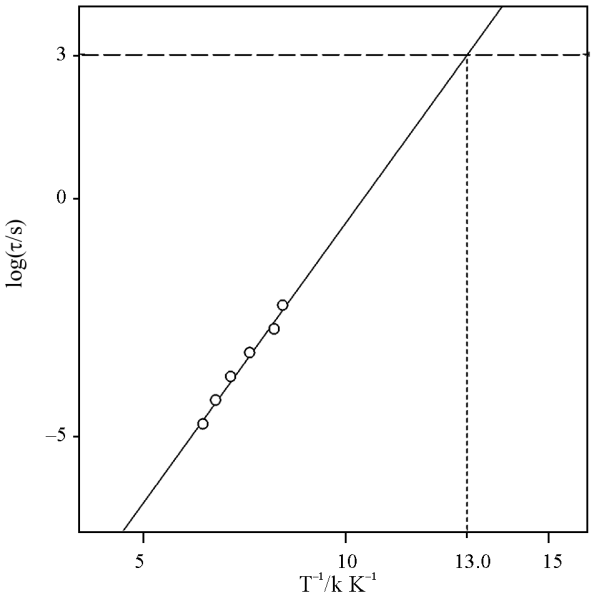

Fig. 7 Arrhenius plot of the dielectric relaxation times,τ's: The data are fitted well by the Arrhenius equation, $\tau=\tau_0\exp(\Delta\varepsilon_a/RT)$, with $\tau_0=4.3\cdot10^{-13}$ s and $\Delta\varepsilon_a$ = 22.6 kJ mol^{-1}

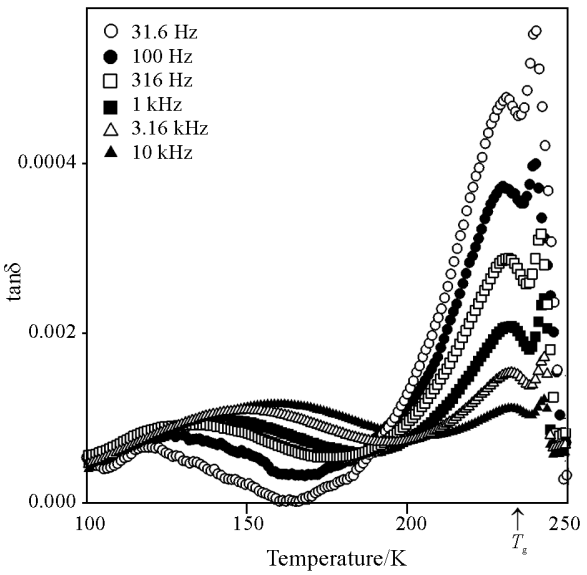

Fig. 6 Dielectric losses of liquid/glass DHBP

Conclusions

Thermal and dielectric relaxation properties of DHBP were disclosed by DSC, adiabatic calorimetry, and dielectrimetry. Crystal nucleation was understood to proceed even at 103 K and crystal growth even at 220 K, indicating the progress of the rearrangement of the whole molecules below the $T_{g\alpha}$=235 K. The β relaxation process was found dielectrically to give its glass transition temperature of $T_{g\beta}$=76.9 K. According to the 'structurally ordered clusters aggregation' model [12, 13], the crystal nucleus can be one of the clusters formed within supercooled liquids/glasses, and the molecules in between the clusters can rearrange above the $T_{g\beta}$ to make the crystal nucleus and to bring the advancement of the crystal surface. 103 K at which the crystal nucleation was indicated to proceed is much above the $T_{g\beta}$. This is reasonable on the assumption of the above model and conversely the model is supported by the results of the present study.

References

1 S. R. Elliott, Physics of Amorphous Materials, Longman, New York 1984.
2 C. A. Angell, J. Non-Cryst. Solids, 131–133 (1991) 13.
3 D. R. Uhlmann, Materials Science Research, Plenum, New York 1969.
4 K. F. Kelton, Solid State Phys., 45 (1991) 75.
5 T. Hikima, M. Hanaya and M. Oguni, Phys. Rev. B, 52 (1995) 3900
6 T. Hikima, M. Hanaya and M. Oguni, Bull. Chem. Soc. Jpn., 69 (1996) 1863.
7 M. Hatase, M. Hanaya and M. Oguni, J. Non-Cryst. Solids, 333 (2004) 129.
8 F. Paladi and M. Oguni, Phys. Rev. B., 65 (2002) 144202.
9 F. Paladi and M. Oguni, J. Phys. Condens. Matter, 15 (2003) 3909.
10 E. O. Schlemper, Acta Cryst., B38 (1982) 1619.
11 K. B. Andersen, M. Langgard and J. Spanget-Larsen, J. Mol. Structure, 509 (1999) 153.
12 H. Fujimori and M. Oguni, Solid State Commun., 94 (1995) 157.
13 M. Oguni, J. Non-Crystalline Solids, 210 (1997) 171.
14 H. Fujimori and M. Oguni, J. Phys. Chem. Solids, 54 (1993) 271.
15 M. Oguni, T. Matsuo, H. Suga and S. Seki, Bull. Chem. Soc. Jpn., 50 (1977) 825.

DOI: 10.1007/s10973-005-7094-9